Journal of Applied Polymer Science

Mechanical and Damping Properties of Epoxy/Liquid Rubber Intercalating Organic Montmorillonite Integration Nanocomposites

Duming Mao, Huawei Zou, Mei Liang, Shengtai Zhou, Yang Chen
The State key Lab. of Polymer Materials Engineering, Polymer Research Institute of Sichuan University, Chengdu 610065, China
Correspondence to: Z. Huawei (E-mail: hwzou@163.com) or L. Mei (E-mail: liangmeiww@163.com)

ABSTRACT: Two different kinds of micro-nanoconstrained damping structure units (M-NCDSUs) were prepared by carboxyl-terminated butadiene acrylonitrile copolymer and epoxy-terminated butadiene acrylonitrile copolymer liquid rubbers intercalating organic montmorillonite, respectively. The prepared M-NCDSUs were then blended with epoxy resin to obtain damping structure integration nanocomposites. The X-ray diffraction and transmission electron microscope measurements applied for the obtained samples confirmed the good formation of M-NCDSUs in the epoxy network. The tensile strength decreased slightly with the addition of M-NCDSUs, whereas the damping properties measured by dynamic mechanical analysis showed a remarkable increase. Besides, the cured epoxy resin exhibited a two-phase morphology where the spherical rubber phase dispersed uniformly in the epoxy matrix. The nanocomposites containing M-NCDSUs showed superior comprehensive properties compared with that without the functional units.
 J. Appl. Polym. Sci. **2014**, *131*, 39797.

KEYWORDS: mechanical properties; nanostructured polymers; structure–property relations; X-ray

Received 5 March 2013; accepted 28 July 2013
DOI: 10.1002/app.39797

INTRODUCTION

With the super high-speed development of contemporary industry, all kinds of machineries are subjected to a mass of vibration and noise that not only deteriorates the life of these devices, but also harms human health. Thus, the damping technology which can be efficient to solve these problems is paid more and more attentions.[1–3]

Since the damping technology came out, many ways have been developed to enhance the damping properties, such as adding plasticizer, interpenetrating polymer network (IPN), alloying, and blending modification. The traditional damping ways may be helpful for increasing damping properties but will significantly sacrifice mechanical properties of the composites. There are two commonly known damping models (Scheme1), which can be simplified as free damping structure and constrained damping structure.[4–6] It is well known that the constrained damping pattern will encounter much larger shear force than the free damping model when suffered from vibration and voices. Consequently, the former will dissipate more vibration energy[7,8] and be crucial to damping properties.

Nowadays, thanks to the development of science and technology, composites with high mechanical properties and superior damping ability can find applications in many areas, such as aircraft, ship, and other structural system.[9] So it is urgent to obtain the damping structure integration material to meet the current needs. However, the problem is it is very hard to enhance the damping capacity while maintaining the corresponding mechanical properties of the composite materials.

Polymer/layered silicate (PLS) nanocomposites have recently aroused intense attention from material investigators for their unique and perfect properties resulted from the combining characteristics of both components at nanometer scale. Moreover, organic montmorillonite (OMMT) has been broadly applied in vast PLS nanocomposites researches for its potentially high surface area and aspect ratio, which lead to the composite materials with relatively enhancement in physical properties.[10] And the intercalated structure of PLS is extremely similar to the macroscopic strained damping structure and sandwich materials.[11–13] Therefore, the PLS technology sheds light on the design of damping structures.

Epoxy resins are widely employed in many industrial applications, such as adhesives, coatings materials, insulating materials in electronic applications and advanced composites for their superior properties in thermal stability, mechanical response, low density, and electrical resistance. However, epoxy resin is known to be brittle while after crosslinking, and thus impairs the physical properties such as impact resistance and tensile strength of the materials.[14] So, in order to meet the requirement

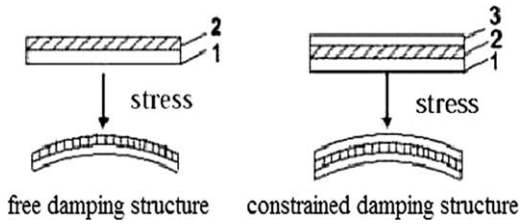

Scheme 1. The schematic illustration of damping structure (one rigid layer, two damping layers, and three constrained layers).

of an advanced composite matrix, a necessary measure has to be carried out. A number of researches have been tried to improve the toughness of epoxy resin. One of the most widespread and effective ways to solve the problem is the addition of liquid rubber.[15] The previous studies have efficiently demonstrated that the addition of liquid rubber into epoxy resin could obtain greatly improvement in fracture toughness.[16,17]

In this study, carboxyl-terminated butadiene acrylonitrile (CTBN) and epoxy-terminated butadiene acrylonitrile (ETBN) copolymers were used as viscoelastic macromolecules that render excellent damping properties,[18] which could be intercalated to the OMMT platelets through intercalation technology, resulting in the formation of micro-nano constrained damping structure units (M-NCDSUs) (Scheme 2)[19] and thus can be classified to the macroscopic constrained damping structure or sandwich structure materials. Then the M-NCDSUs were mixed with epoxy resin, and the consequently curing composites were obtained as the damping structure integration nanocomposites.

EXPERIMENTAL

Raw Materials

The OMMT which was modified with octadecyltrimethylammonium bromide was provided by America Nanocor. CTBN and ETBN which were used as viscoelastic macromolecules were supplied by America Emerald and Beijing Devote Chemical, China, respectively. The detailed molecular formulas for the liquid rubbers were shown in Scheme 3. Polypropylene glycol diglycidyl ether (DER732) was employed as the diluent of liquid rubbers which was purchased from Dow Chemicals. Diglycidyl ether of bisphenol A-based (DGEBA) epoxy resin E-51with an epoxy value of 0.51 was obtained from Jiangsu Wuxi Resin Plant, China. 4,4-diamino diphenyl methane (DDM) as curing agent was purchased from Shanghai SSS Reagent, China.

Synthesis of M-NCDSUs

A certain amount of DER732 and CTBN (or ETBN) were poured into a glass beaker, then heated to 120°C and stirred drastically to intercalate with a predetermined amount of OMMT. The intercalation process was undergone with the conditions of vigorously stirred for about 90 min at 120°C to form the M-NCDSUs.[20]

Preparation of Epoxy/M-NCDSUs Nanocomposites

Five series of samples containing CTBN, ETBN, and OMMT were prepared according to the procedures reported by Tripathi et al. and Jia et al.[21,22] The detailed formulations were illustrated in Table I. The preparation section of the composites followed five consecutive steps: firstly, the calculated quantity epoxy resin was stirred at 120°C for half an hour to remove the air bubbles. Subsequently, the prepared M-NCDSUs were added and the resultant mixture was stirred at 120°C for 60 min. However, for fear of the formation of intercalation units in the nonintercalation systems, the added DER732, ETBN, and OMMT were stirred at 120°C for 15 min. Thirdly, 28 phr DDM was fed into the mixture and mixed at 80°C for another 10 min. For the exfoliation sample E-EPE35, firstly, the calculated quantity epoxy resin and OMMT were stirred at 120°C for 60 min, then 28 phr DDM was fed into the mixture and mixed at 80°C for another 10 min, thirdly, DER732 and ETBN were added and stirred at 80°C for 15 min. Finally, the mixture was degassed under a vacuum for 20 min, and then poured into the preheated Teflon molds to make dog-bone shaped samples for further characterizations. Consequently, the filled molds were put into hot air oven, which was heated from room temperature to 135°C

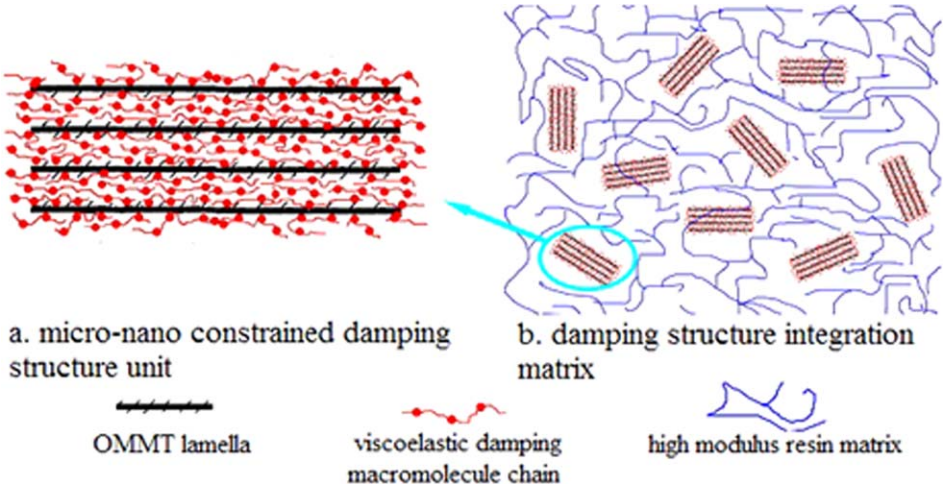

Scheme 2. The schematic illustration of micro-nanoconstrained damping structure integration material: (a) micro-nanoconstrained damping structure unit and (b) damping structure integration matrix. [Color figure can be viewed in the online issue, which is available at wileyonlinelibrary.com.]

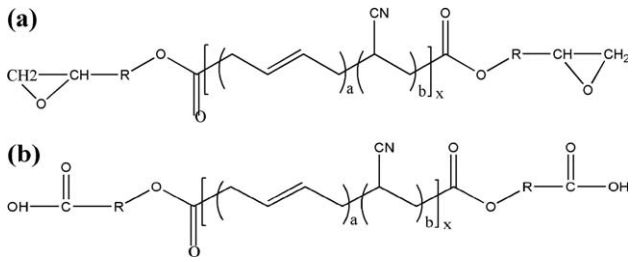

Scheme 3. The molecular formulas of liquid rubbers: (a) ETBN and (b) CTBN.

and cured for 2 h, then postcured for 2 h at 175°C to obtain the expected nanocomposites.

Characterization

X-ray Diffraction Analysis. X-ray diffraction (XRD; DY1291, Philips, Holland) measurements on the powder, liquid M-NCDSUs, and cured epoxy plates were performed by a D/MAX-III power diffractometer with wavelength 0.1542 nm of Cu Kα. The XRD was performed in the 2θ angle range from 1.5° to 15° at room temperature.

The interlayer spacing between OMMT layers in the matrix was calculated by using the classic Bragg's equation:

$$n\lambda = 2d\sin\theta \quad (1)$$

where λ represents the wavelength of the X-ray source, θ is the diffraction angle, and d is the spacing between diffractional lattice planes (001).[23]

Transmission Electron Microscope Analysis. The nanoscale structure of the intercalated M-NCDSUs in the epoxy network was observed by a transmission electron microscope (TEM; Tecnai G^2 F20, FEI, USA) inspection with an acceleration voltage of 120 kV. The ultrathin sections with a thickness of 100 nm were cryogenically microtomed by using an ultra-microtome (EM UC7, LEICA, Germany).

Mechanical Analysis. The tensile strength was performed with the help of Instron (Instron 5567; Instron, USA) universal testing instrument at 10 mm/min according to ASTM D-638. The values were taken from an average of five specimens.

Dynamic Mechanical Analysis. The glass transition temperatures (T_g) of cured samples were determined by dynamic mechanical analysis (DMA; Q800, TA, USA) instrument. It is a well-known method for determining viscoelastic properties by applying a controlled sinusoidal strain to tested sample and measuring the resultant stress. DMA gives storage modulus characteristics as a function of temperature. The peak area of the DMA curve which is used to evaluate the damping properties is calculated by the origin software. The measurements were carried out at a heating rate of 3°C/min from 30 to 220°C at fixed frequency of 1 Hz. The samples were rectangular bars of sizes 20 mm×10 mm×4 mm.

Table I. Compositions in Parts Per Hundred of Epoxy Resin for Each Component in the Final Materials

Sample	Epoxy (%)	DER732-CTBN/OMMT=8/2(%)	DER732-ETBN/OMMT=8/2(%)
EP0	100	0	0
EPC35	65	35	0
EPE35	65	0	35 (Intercalation units)
epe35	65	0	35 (Nonintercalation units)

Scanning Electron Microscopic Analysis. The surface morphology of the composites was observed by a scanning electron microscope (SEM; JSM-5900, JEOL, Tokyo, Japan) instrument with an acceleration voltage of 5 kV. The samples were cryogenically fractured in liquid nitrogen, and all of the fractured surfaces were coated with gold to enhance the image resolution and to prevent electrostatic charging.

RESULTS AND DISCUSSION

Influence of Different M-NCDSUs on the Composite Performances

XRD Results of Different Liquid Rubbers Intercalating OMMT. Figure 1 shows the XRD spectra of OMMT, M-NCDSUs, and M-NCDSUs modified epoxy resins. It is clearly seen in [Figure 1(a)] that the interlayer spacing between OMMT layers was 2.13 nm. Those of DER732-CTBN/OMMT units showed two peaks. A main peak at 3.71 nm and a secondary diffraction peak ($n\lambda = 2d\sin\theta$, $n = 2$) at 1.83 nm were observed. In the case of most nanocomposite systems, the higher order peaks observed around 1.83 nm correlates to the (002) plane and therefore represents only half the distance of the $d_{(001)}$-spacing.[24] Concurrently, a similar result was observed in the DER732-ETBN/OMMT units for their similar molecular formula. These results clearly demonstrated that during the intercalation process, liquid rubbers were successfully intercalated into the layers of OMMT and the M-NCDSUs were obtained as expected.[25] However, the characteristic peaks were existent but blurry in epoxy/liquid rubber intercalating OMMT composites, as were clearly shown in Figure 1(b). It could be conjectured that the silicate layers were further intercalated by epoxy resin and curing agent DDM, and then exfoliated partly during the courses of vigorous stirring and subsequent polymerization.[26] Then the regular OMMT lamellas were appulsively transformed into random structures. The results indicate that the M-NCDSUs still existed in the composites.

In addition, the interlayer spacing of sample EPE35 was slightly wider than sample EPC35. Based on the work by Lan et al. and Kornmanna et al.[27,28], the polymerization was believed to be the indirect driving force of the exfoliation, and a balance between the intragallery and the extragallery polymerization rates was required in order to exfoliate the clay in epoxy systems. In our experiments, the ETBN was easier to react with the curing agent than the CTBN, so we could infer that the intragallery polymerization rates in ETBN system was faster than in CTBN system. As a conclusion, the ETBN system should own larger interspacing than the CTBN system.

The TEM images of sample EPE35 are shown in Fig.2 and Fig.3, respectively. These solid dark lines in the images, corresponding to the silicate mono-layers, demonstrate intercalated structure of M-NCDSUs, which is consistent with the results of

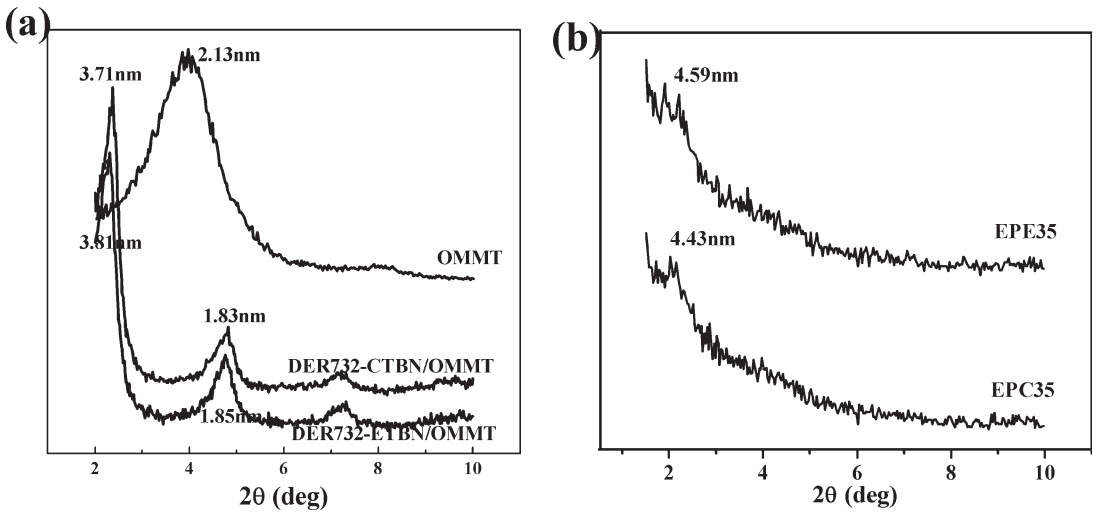

Figure 1. X-ray diffractometer patterns of polymer-layered silicate: (a) liquid rubbers intercalating OMMT and (b) intercalating nanocomposites.

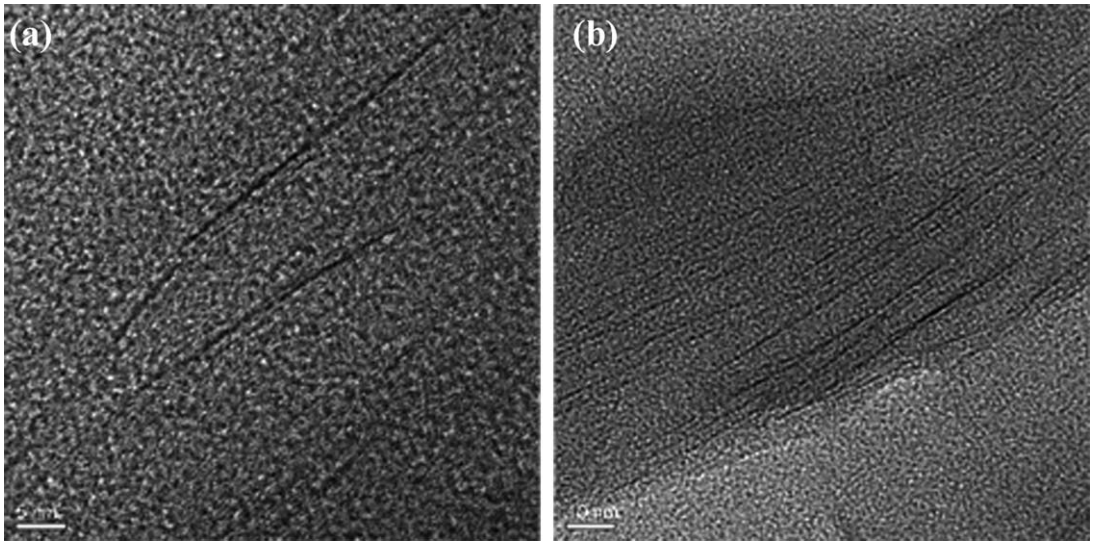

Figure 2. TEM images of sample EPE35 in different magnifications (5 and 10 nm).

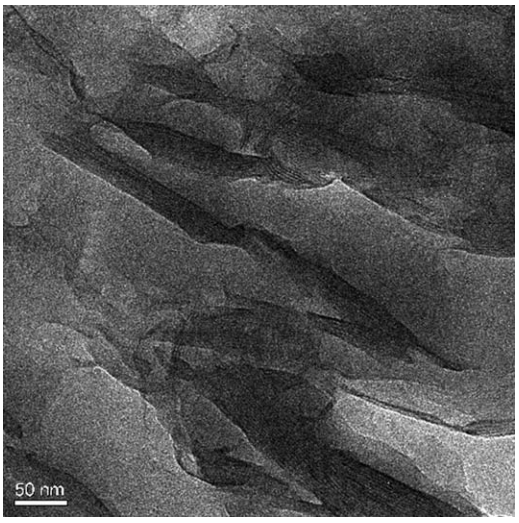

Figure 3. TEM images of sample EPE35 (50 nm).

XRD analysis.[29] Although the layer spacing increased, the silicate layers still maintained ordered stacks in the epoxy/M-NCDSUs nanocomposites. However, OMMT tactoids were not obviously existed because of its homogeneous dispersion. The TEM images validly confirmed that the M-NCDSUs were well maintained in the epoxy network.

Influence of Different m-NCDSUs on Mechanical Properties of Composites

Tensile strength is plotted with the variation of M-NCDSUs in the blends and has been shown in Figure 4. A reasonable decrease in tensile strength was notably observed with the addition of liquid rubber intercalating OMMT units. It is clearly seen in Table II that the mechanical properties decrease and the damping properties increase with the content of M-NCDSUs increase. This might be ascribed to the existence of the relative amount of dissolved rubber as the addition of M-NCDSUs. It was a well-known phenomenon that the existence of dissolved

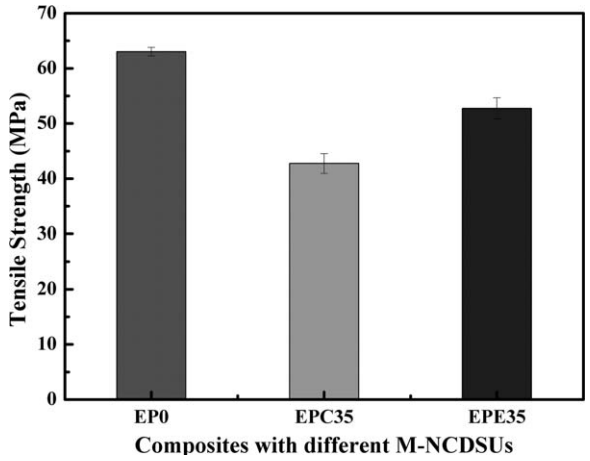

Figure 4. The tensile properties for composites with different M-NCDSUs.

rubber would severely weaken the tensile strength of the nanocomposites. However, the tensile strength was much higher than the other research literatures' with 35 phr liquid rubber who was under 10 MPa.[21] This behavior might be interpreted that the OMMT lamellas could notably strengthen tensile strength, which is known as the nano-enhancement effect. When struck a balance between dissolved rubber and the nano-enhancement effect, the samples containing damping structure units (M-NCDSUs) came to be the ideal option.

The results of the mechanical properties also indicated that the cured epoxy resin containing ETBN was much better in the tensile properties than the CTBN system. It could be illustrated that the epoxide groups of ETBN were more apt to react with the curing agent DDM when compared with the carboxyl groups of CTBN at the same reaction conditions. Therefore, the former could form more linkages between liquid rubber ETBN and epoxy network than CTBN, leading to a fact that EPE35 samples demonstrated better mechanical properties.

Influence of Different M-NCDSUs on Damping Properties of Composites

Figure 5(a) shows the tan δ, T_g and peak area for epoxy resin/DDM with the variation of M-NCDSUs. The glass transition temperature T_g, taken at the maximum of the value tan δ curve at 1 Hz, was 189.9°C for epoxy resin cured with DDM, which was much higher than the values for other systems. It can be drawn in Figure 5(a) that the T_g s of samples EPC35 and EPE35

Table II. Influence of M-NCDSUs Content on Mechanical Properties of Composites

Sample	Tensile Strength (MPa)	Peak Area	T_g (°C)
EPE0	63.04	12.54	189.90
EPE10	60.59	16.22	168.31
EPE20	57.34	18.91	145.39
EPE30	54.03	21.73	115.04
EPE35	52.76	25.00	84.62
EPE40	35.28	31.65	41.58

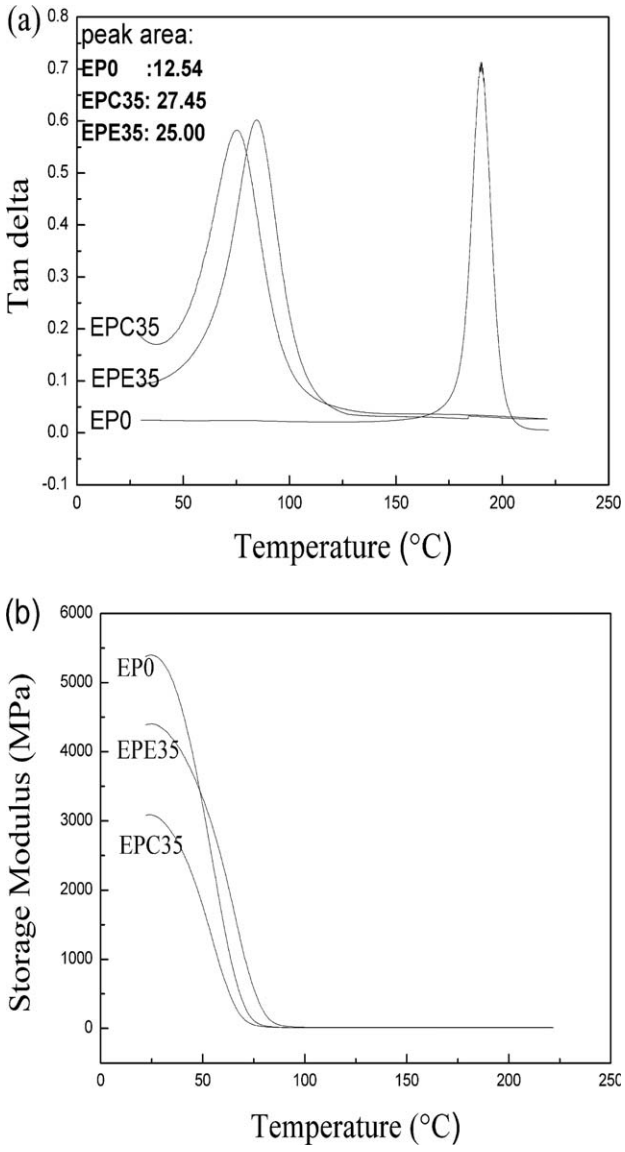

Figure 5. (a) Variation in the values of tan δ of prepared samples with temperature. (b) Variation of storage modulus with temperature of prepared samples.

were 75.4°C and 84.6°C, respectively. The addition of M-NCDSUs in the matrix greatly decreased the T_g of the epoxy matrix by about 110°C. The difference in the T_g s might be because of the fact that the filled materials were not fully cured or that some of the liquid rubber was dissolved in the epoxy phase and was plasticizing the glass transition.[21]

On the basis of the peak area in Figure 5, sample EPC35 showed the best damping properties, and sample EPE35 was also superior to the neat epoxy matrix EP0. This might be attributed to the higher damping characteristic of viscoelastic macromolecules than the rigid epoxy resin. In light of the formula of both viscoelastic macromolecules (Scheme 3), ETBN could readily react with the curing agent DDM, thus leading to the formation of a much denser network between ETBN and epoxy than the CTBN system, which slightly deteriorates the damping properties of the nanocomposites.

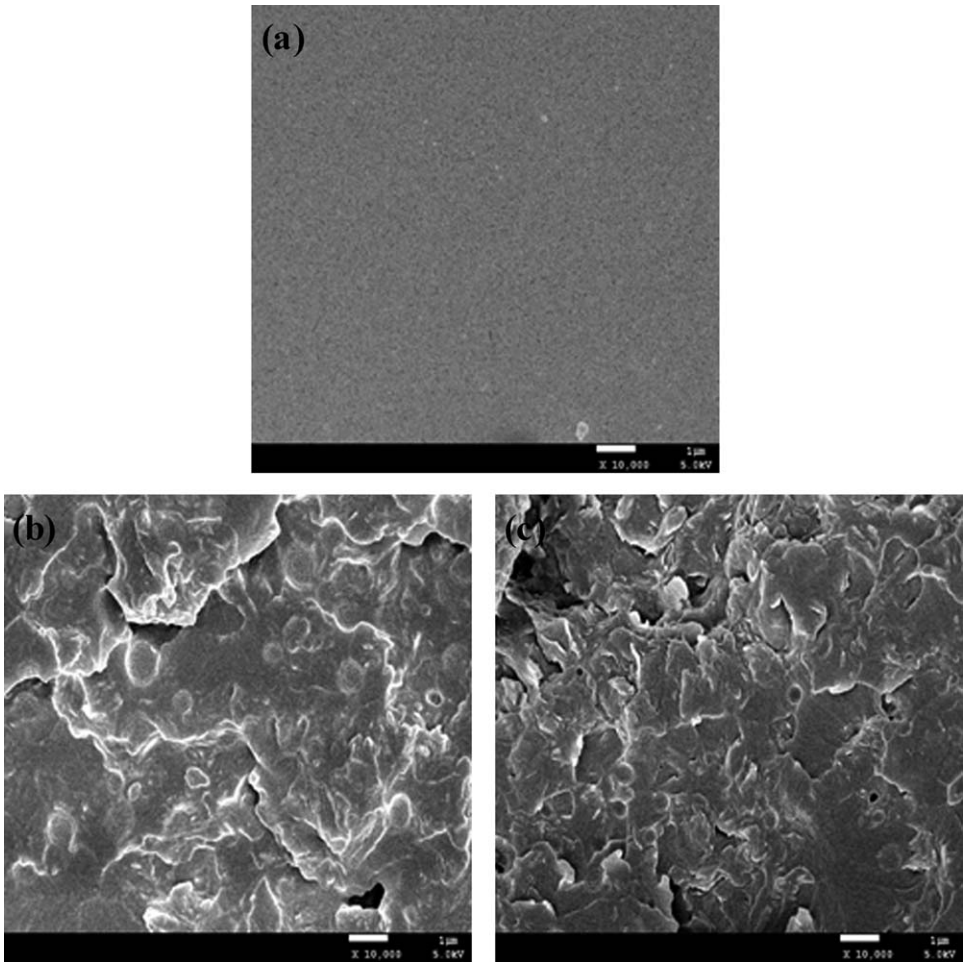

Figure 6. SEM photos for the epoxy/M-NCDSUs blends: (a) EP0, (b) EPC35, and (c) EPE35.

A gradual drop of storage modulus with the addition of M-NCDSUs revealed the increased flexibility of the blend samples. Sample EPC35 showed maximum flexibility [Figure 5(b)]. The stiffness of the resultant material was also temperature sensitive. The storage modulus dropped with increasing temperature indicated that all formulations gradually passed from stiff hard solid to soft and flexible material that agrees well with previous reasoning. Similar results have been reported by Tripathi et al. and Jia et al.[21,22] for epoxy terminated butadiene/acrylonitrile rubber in an aromatic amine cured DGEBA epoxy.

Influence of Different M-NCDSUs on Scanning Electron Microscope of Composites

Representative SEM micrographs of the cryogenically fractured surface of the unmodified and M-NCDSUs-modified epoxy matrix are shown in Figure 6(a–c). The pattern of morphology observed for the unmodified formulation [Figure 6(a)] was the characteristics of brittle systems, which presented a smooth and glassy fractured surface in the plane. SEM micrographs of CTBN-modified systems showed that the precipitated rubber particles dispersed discretely in the epoxy matrix. The results implied the presence of two-phase morphological feature or typically "sea-island" structure, which has a prominent contribution to the damping properties of the obtained systems. The soft rubber phase was the liquid rubber separated from the rigid epoxy matrix during the early stage of cure.[30] Furthermore, a similar result was also observed in sample EPE35 [Figure 6(c)]. The particle size of the rubber phase was larger in EPC35 than that in EPE35. This might be related to the re-agglomeration of the randomly dispersed dissolved rubber particles. However, other than CTBN, ETBN could react with the curing agent DDM. Therefore, there was more dissolved rubber in sample EPC35 than sample EPE35, which had a flexibilization effect on the matrix, resulting in the reduction of mechanical properties.

Influence of Different Units on Properties of Composites

Figure 7(a) shows the XRD spectra of nonintercalation units in the composites. The interspacing between OMMT layers in the nonintercalation system increased from 2.13 to 2.45 nm, and the interspacing of cured N-EPE35 was only 2.54 nm. In contrast, the interlayer spacing in the nonintercalation system was much smaller than the intercalation system shown in (Figure 1(b), which could be conjectured that

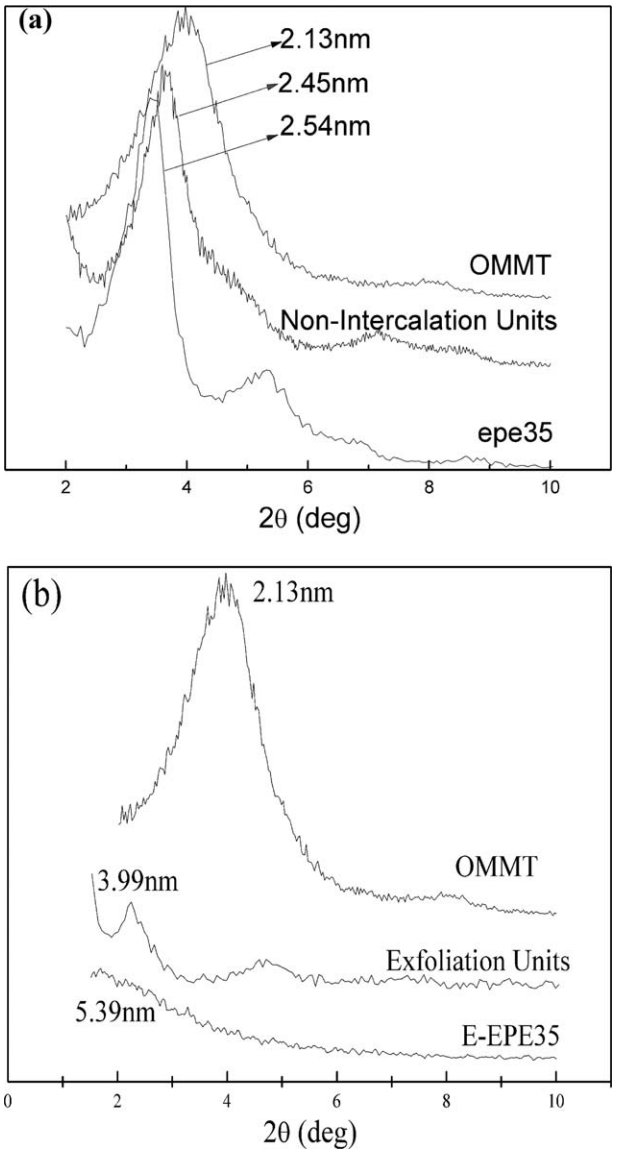

Figure 7. (a) X-ray diffractometer (XRD) patterns of samples (a) N-EPE35 and (b) E-EPE35.

there was not enough time in the blending process of sample N-EPE35 to form the well-constructed intercalation units. Figure 7(b) shows the XRD spectra of exfoliation units in the composites. The interspacing between OMMT layers in exfoliation system increased from 2.13 to 3.99 nm, and there was only weak and blurry interspacing in the cured N-EPE35 that could be considered as the exfoliaton system.[31]

Tensile strength is plotted against the variation of intercalation, exfoliation, and nonintercalation units in the composites, which was shown in Figure 8. A remarkable decrease in tensile strength was notably observed with the addition of nonintercalating units, which can be ascribed to the existence of relative amount of agglomerate OMMT in composite with nonintercalation units. This was also a common and known fact that agglomerate phenomenon would

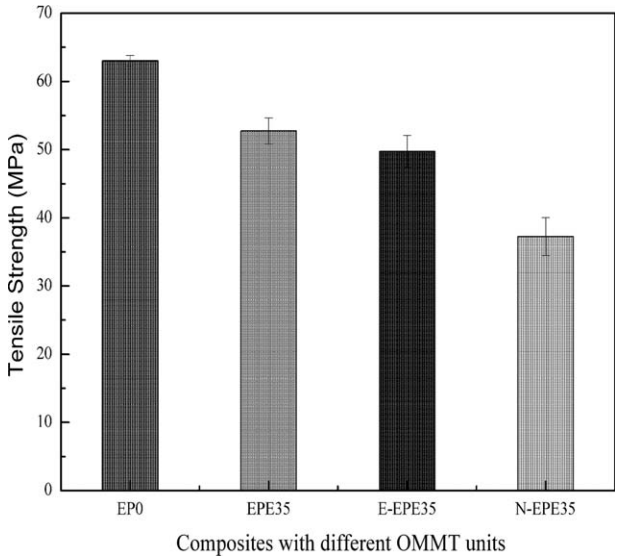

Figure 8. Tensile properties for composites: EP0, EPE35, E-EPE35, and N-EPE35.

severely weaken the tensile strength of the blends.[22] And the tensile strength of sample E-EPE35 was slightly inferior to the sample EPE35. In general, the exfoliation system owns much better mechanical performances than intercalation system or nonintercalation system. But in our experiments, most of the epoxy resins were constrained instead of liquid rubber, and liquid rubber was negative to mechanical performances.

Figure 9 shows the DMA data for epoxy resin with intercalation and nonintercalation units. The T_gs of EPE35 and epe35 were 84.6°C and 78.35°C, respectively. The difference in T_gs might be solely because of the barrier effect of OMMT lamellas on the molecular motion which was confined by the OMMT lamellas.[32] Furthermore, T_g is related to the molecular motion, and the barrier effect in intercalated sample was stronger than in the nonintercalated sample for the former demonstrated much larger interlayer spacing.

The peak area of DMA curves were also shown in Figure 9(a), sample EPE35 presented the best damping properties among these samples. As expected, the results might be explained by the classical theory that the intercalation system just like the macroscopical constrained damping structure can induce higher damping characteristics than the nonintercalation and exfoliation system, which is similar to the free damping structure. However, the difference of damping properties between the intercalation and nonintercalation systems was not very noticeable because the internal friction between OMMT lamellas and epoxy matrix in nonintercalation system was stronger than that in intercalation system. Meanwhile, the internal friction played a very significant role in dissipating the vibrating energy to enhance the damping properties of the nanocomposites.[33–35] Because the constraint and internal friction effect of E-EPE35 was inferior to the EPE35 and N-EPE35, E-EPE35 owned the worst damping performance.

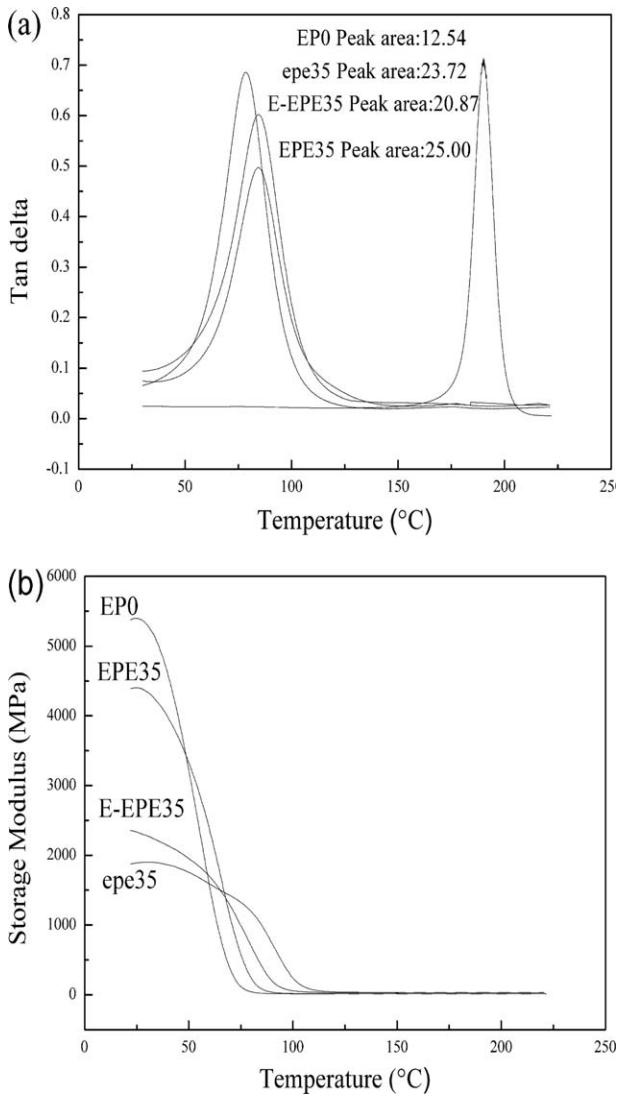

Figure 9. (a) Variation of damping peak area of prepared samples with temperature. (b) Variation of storage modulus with temperature of prepared samples.

The storage modulus decreased with the addition of different OMMT units in Figure 9(b). And the tensile strength and storage modulus of different samples had the same variation trend.

CONCLUSIONS

In this study, epoxy resin was toughened by the addition of CTBN- and ETBN-intercalated OMMT units, respectively. XRD and TEM measurements confirmed the good intercalation of viscoelastic macromolecules. There were a sharp reduction in T_g and a remarkable improvement in damping properties with the addition of M-NCDSUs into epoxy matrix, whereas the tensile strength showed a slight reduction for the enhancement of OMMT nanolamella. As a comparison, the mechanical properties of ETBN samples were superior to that of CTBN samples for the difference of their functional groups. Furthermore, a comparison among the intercalation, nonintercalation, and exfoliation systems illustrated that M-NCDSUs played a significant role in comprehensive properties of the nanocomposites.

ACKNOWLEDGMENTS

The authors would like to thank National Natural Science Foundation of China (51273118), Provincial Science and Technology Pillar Program of Sichuan (2013FZ0006), and Program of JPPT-115-5-1716 for financial support, and thank Analytical and Testing Center of Sichuan University for Providing XRD, TEM, and SEM measurements.

REFERENCES

1. Wang, T.; Chen, S.; Wang, Q.; Pei, X. *Mater. Des.* **2010**, *31*, 3810.
2. Remillat, C. *Mech. Mater.* **2007**, *39*, 525.
3. Adams, R. D.; Maheri, M. R. *J. Alloy Compd.* **2003**, *355*, 126.
4. Bamberg, E.; Slocum, A. *Precis. Eng.* **2002**, *26*, 430.
5. Buravalla, V. R.; Remillat, C.; Rongong, J. A; Tomlison, G. R. *Mater. Res. Bull.* **2001**, 2001, 10.
6. Vuure, A.W.; Verpoest, I.; Ko, F. K. *Compos. Part. B Eng.* **2001**, *32*, 11.
7. Meunier, M; Shenoi, R. A. *Compos. Struct.* **2001**, *243*, 54.
8. Berthelot, J.; Assarar, M.; Sefrani, Y.; Mahi, A. *Compos. Struct.* **2008**, *85*, 189.
9. Yu, L.; Ma, Y.; Zhou, C.; Xu, H. *Int. J. Solids Struct.* **2005**, *42*, 3045.
10. Kiliaris, P.; Papaspyrides, C. D. *Prog. Polym. Sci.* **2010**, *35*, 902.
11. Barkanov, E.; Skukis, E.; Petitjean, B. *J. Sound Vib.* **2009**, *327*, 402.
12. Ray, S.; Okamoto, M. *Prog. Polym. Sci.* **2003**, *28*, 1539.
13. Yadav, B. *J. Sound Vib.* **2008**, *317*, 576.
14. Chen, S.; Wang, Q.; Wang, T. *Polym. Test.* **2011**, *30*, 726.
15. Lin, C.; Wang, Y.; Feng, Y.; Wang, M.; Juang, T. *Polymer* **2013**, *54*, 1612.
16. Dadfar, M. R.; Ghadami, F. *Mater. Des.* **2013**, *47*, 16.
17. Balakrishnan, S.; Start, P. R.; Raghavan, D. *Polymer* **2005**, *46*, 11255.
18. Sher, B. R.; Moreira, R. A. S. *Compos. Struct.* **2013**, *99*, 241.
19. Alexandre, M.; Dubois, P. *Mater. Sci. Eng. R.* **2000**, *28*, 1.
20. Zhua, S.; Chena, J. *Appl. Surf. Sci.* **2013**, *264*, 500.
21. Tripathi, G.; Srivastava, D. *Mater. Sci. Eng. A.* **2007**, *443*, 262.
22. Jia, Q.; Zheng, M.; Chen, H.; Jia, R. *Mater. Lett.* **2006**, *60*,1306.
23. Zhang, H.; Shi, C.; Han, J.; Yu, J. *Constr. Build. Mater.* **2013**, *40*, 1151.

24. Masami, O.; Satoshi, M.; Hideyuki, T. *Polymer* **2000**, *41*, 3887.
25. Wanga, B.; Qi, N.; Gonga, W.; Li, X.; Zhen, Y. *Radiat. Phys. Chem.* **2007**, *76*, 146.
26. Guo, B.; Jia, D.; Cai, C. *Eur. Polym. J.* **2004**, *40*, 1743.
27. Lan, T.; Kaviratna, P. D; Pinnavaia, T. J. *Chem. Mater.* **1995**, *7*, 2144.
28. Kornmanna, X.; Lindbergb, H.; Berglund, L. A. *Polymer* **2001**, *42*, 4493.
29. Zhao, L.; Li, J.; Guo, S.; Du, Q. *Polymer* **2006**, *47*, 2460.
30. Ratna, D. *Polymer* **2001**, *42*, 4209.
31. Suprakas, S. R.; Masami, O. *Prog. Polym. Sci.* **2003**, *28*, 1539.
32. Ozcalik, O.; Tihminlioglu, F. *J. Food Eng.* **2013**, *114*, 505.
33. Seiner, H.; Sedlák, P.; Koller, M. *Compos. Sci. Technol.* **2013**, *75*, 93.
34. Zaykin, Y.; Koztaeva, U. P. *Radiat. Phys. Chem.* **2000**, *58*, 387.
35. De, D.; Panda, P.; Roy, M.; Bhunia, S. *Mater. Des.* **2013**, *46*, 142.